Comparative Examination of Control Strategies in DC-DC Power Converters: A Traditional and Artificial Intelligence Perspective

Erik Martínez-Vera[1]*, Pedro Bañuelos-Sánchez[1], Gibrán Etcheverry[2]

[1] Intelligent Systems, Universidad de las Américas-Puebla, 72810 San Andrés Cholula, Mexico
[2] Intelligent Systems, Tiffin University, 44883 Tiffin, USA

* Correspondence: Erik Martínez-Vera (erik.martinezva@udlap.mx)

Citation: E. Martínez-Vera, P. Bañuelos-Sánchez, and G. Etcheverry, "Comparative examination of control strategies in DC-DC power converters: A traditional and artificial intelligence perspective," *J. Intell Syst. Control*, vol. 2, no. 2, pp. 82–98, 2023. https://doi.org/10.56578/jisc020203.

Abstract: This study undertakes a comprehensive review of control techniques applicable to DC-DC power converters, categorized into Traditional Control (TC) methods and those based on Artificial Intelligence (AI). Succinct descriptions of prevalent strategies in both classifications are furnished, shedding light on their fundamental principles. Further, the current progress in the field is evaluated, anchoring the discussion in the provided categorization. In assessing the merits and potential drawbacks of each method, specific emphasis is laid on the target converter topology. Predominant topologies such as the elementary buck, boost, bidirectional buck-boost, and dual-active-bridge (DAB) are scrutinized. To furnish a thorough analysis and facilitate comparison of principal control methods, simulations of four fundamental off-the-shelf algorithms are undertaken, employing a 1 MHz switching frequency.

Keywords: DC-DC converters; Control; Artificial intelligence

1 Introduction

Power converters play a crucial role in modern electronics, serving as interfaces between energy sources and loads. They are essential in numerous applications, such as telecommunications, personal computers, aircraft, and electric vehicles. Converters can be categorized based on the type of input and output energy, including AC-DC (rectifiers), DC-DC, DC-AC (inverters), and AC-AC. Present research focuses on developing efficient devices with high power density and low cost. Various circuit topologies enable a reduction in component count while extending the output voltage range. Emerging semiconductor materials, such as Silicon Carbide (SiC) and Gallium Nitride (GaN), offer higher switching frequencies than traditional silicon (Si) power switches, enabling a decrease in passive component sizes. As converters are used in dynamic systems, precise regulation is crucial during power transients to prevent damage to the converter components and, more importantly, the loads. Consequently, reliable and accurate control methods are required for proper system operation and component safety. This work aims to conduct a comprehensive review of control methods for DC-DC power converters.

A meaningful classification of control methods was derived from an analysis of a sample of papers drawn from various journals. For each paper, the control type and circuit topology were documented. It was observed that the control type is dependent on the circuit topology, with simpler control methods for elementary topologies and more complex methods for topologies involving a larger number of components. Furthermore, the control technique varies based on the number of inputs and outputs. Single input-output systems may employ a single feedback loop, while multi-input/output topologies necessitate additional loops to regulate simultaneous power flow from multiple sources. Figure 1 presents the control methods versus normalized frequency for the reviewed papers. The most commonly identified methods were Proportional-Integral-Derivative (PID), Neural Network Control (NN), and Fuzzy Logic Control (FL), with Model Predictive Control (MPC) and Sliding Mode Control (SMC) also being applied. Based on these findings, a classification is proposed, dividing control methods into Traditional Control (TC) and Artificial Intelligence (AI) control.

A flow diagram for the review is proposed in Figure 2. PID, MPC, and SMC represent the primary methods within the TC category, while NN and FL constitute the main methods for the AI category. Less frequently employed control techniques are classified into the "others" category for both groups. Therefore, this work contributes by
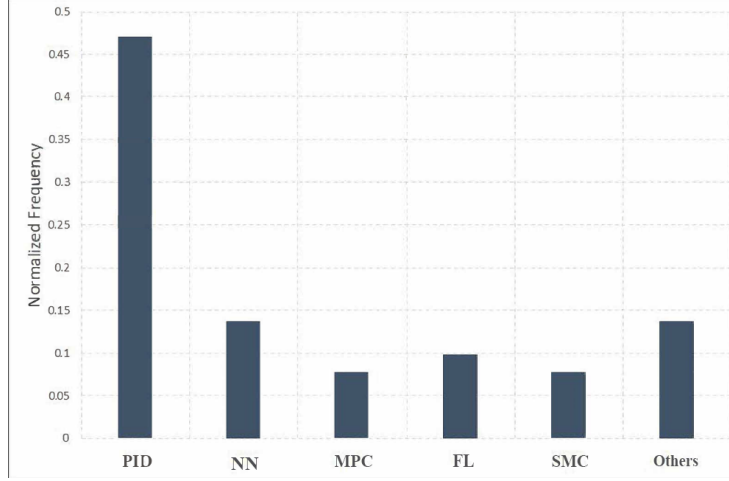
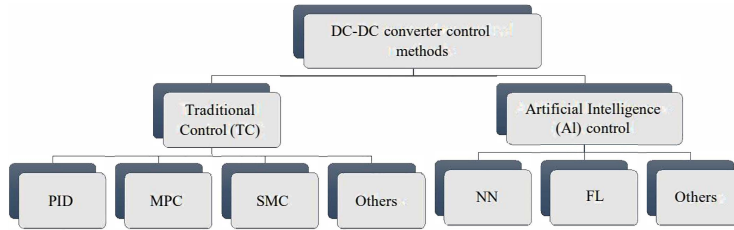**Figure 1.** Control methods vs normalized frequency

Figure 2. Proposed classification of control methods

offering insight into the control techniques currently applied to DC-DC converters, enabling the identification of methods, scope, and limitations of existing research. By recognizing trends in the state-of-the-art, directions for future research can be defined.

The examination of the structure of power converters, their functioning, and control methods, along with an analysis of current research trends, provides a significant basis for further investigation. With a focus on TC and AI control methods, the review seeks to contribute to an understanding of how DC-DC converters function, their current limitations, and future directions for improvement. As such, it provides a comprehensive starting point for future researchers and professionals in the field.

2 Traditional Control Methods Methodology

2.1 PID

The prevalent control methodology employed in industrial applications is the Proportional Integral Derivative (PID), revered for its implementation simplicity and functional adaptability even in the absence of a comprehensive plant model [1]. This approach continues to be the gold standard against which emerging techniques are measured.

Figure 3 delineates the block diagram associated with PID control. The input of the PID block, denoted as e, is characterized as the discrepancy between the output voltage of the converter (V_{out}) and the desired reference voltage (V_{ref}). The control action u is mathematically represented in Eq. (1), wherein K_p denotes the proportional gain, T_i signifies the integral time, and T_d corresponds to the derivative time [1].
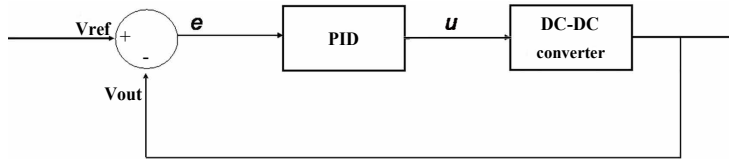

Figure 3. Block diagram of PID control

$$u(t) = K_p e(t) + \frac{K_p}{T_i} \int_0^t e(t)dt + K_p T_d \frac{de(t)}{dt} \qquad (1)$$

The implementation of PID in DC-DC power conversion has been witnessed across various sectors such as railway systems [2], electric vehicles [3–10], grid power flow control [11], microgrids [12], and communication systems [13], to name a few. Its inherent simplicity enables effective integration with high-frequency SiC and GaN switching topologies [2, 10].

The control schematic depicted in Figure 3 pertains to Voltage Mode Control (VMC), typically employed in single input/single output converter configurations [2, 11]. To regulate power flow in multiple input/output topologies, PID blocks can be employed in parallel [3, 8].

One of the challenges posed by an aggressive PID control action is the resultant high peak currents. To mitigate this, an additional feedback loop is used to control the inductor current, which is defined as Current Control Mode (CMC). This auxiliary loop facilitates faster converter action while avoiding excessive current peaks [9, 14]. Topologies with multiple input/outputs leverage PID blocks in cascade and parallel configurations to achieve VMC or CMC [4–6, 10, 12].
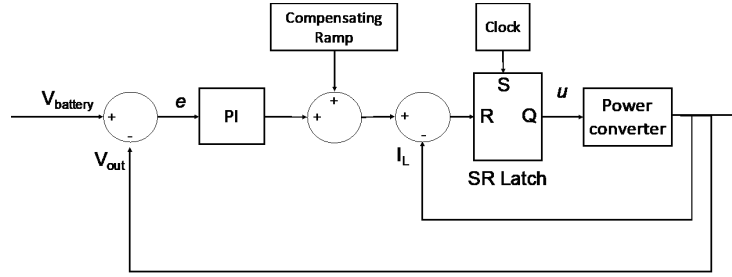

Figure 4. PI with CMC control [4]

Figure 4 exhibits PI-CMC control employed for a hybrid energy storage system involving a battery and an ultra-capacitor (UC) [4]. An example of the application of four parallel control loops with proportional integral (PI) blocks for a flyback DC-DC converter is shown in Figure 5. Isolated topologies utilize phase-shift to regulate power transfer [10]. Due to the high sensitivity of the derivative term in PID control, it is often omitted [15].
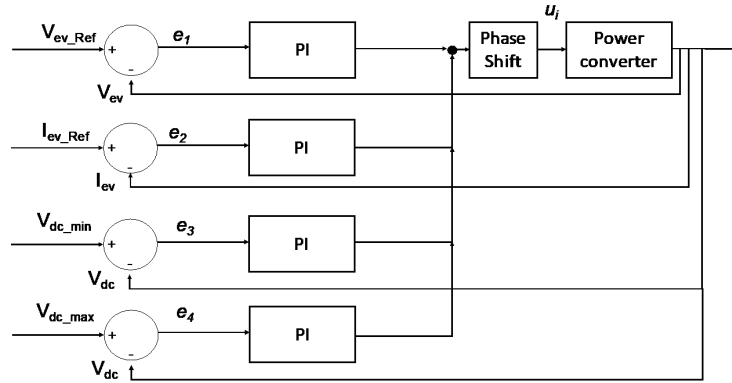

Figure 5. Parallel PI control loops [10]

Experimental validation of PID for DC-DC converters has been demonstrated using microcontrollers [6, 7] or FPGAs [11, 16]. Apart from serving as the benchmark, PID control has also been integrated with other control techniques, as will be outlined in subsequent sections.

The broader implications of this study extend to the fields of power electronics and control systems, providing an enhanced understanding of traditional control methods' utility and potential for further refinement. Further elaboration on this topic will include a comparative analysis of PID with other control techniques and exploration of the potential for hybrid solutions.

2.2 Model Predictive Control

The MPC strategy operates based on a model that forecasts a sequence of output voltages, taking into account the present output and duty cycle. The prognosticated output values are juxtaposed with the desired reference, facilitating the calculation of the forecasted discrepancy. To minimize the objective function within set parameters, an optimal control action needs to be identified [17].

MPC control is depicted in Figure 6 via a block diagram. The objective function is commonly represented as:

$$J = \sum_{j=0}^{N-1} \left(\left\| V_{ref} - \left(V_{outk+j|k} - \hat{d}_k \right) \right\|_Q^2 + \left\| \Delta u_{k+j|k} \right\|_S^2 \right) \tag{2}$$
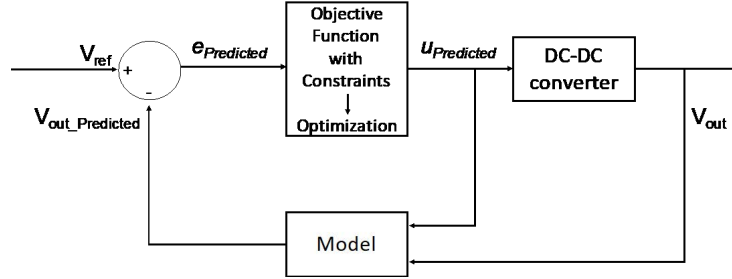

Figure 6. Block diagram of MPC control

where, N denotes the prediction horizon, with the subscript $k + j|k$ implying prediction up to time j, including time k. Matrices Q and S serve as the weighting factors. The term $\hat{d}_k$ represents the discrepancy between the converter's output and the model prediction at time k.

A model of the converter is indispensable for prognosticating future values. Although precise models offer superior predictions, they come with the trade-off of increased intricacy. A comparison with the simpler PID model (Eq. (1)) reveals the heightened complexity of MPC, leading to additional computational demands. Notwithstanding, in terms of performance, MPC achieves steady-state more rapidly and avoids voltage overshoots compared to the PID model [18, 19]. Moreover, the restrictions imposed on the objective function facilitate current control without necessitating additional feedback loops [20].

An attempt to circumvent the cumbersome process of online model prediction and optimization led to the emergence of explicit MPC. It evaluates offline all potential control actions and archives them in a table. However, these tables can be voluminous, and trawling through them for the appropriate duty cycle can be arduous and time-consuming. Consequently, MPC has been coupled with neural networks, enabling explicit MPC to operate at exceedingly high switching frequencies [21, 22].

This analysis underscores the benefits and challenges of the MPC strategy. While it has proven effective, there are still obstacles to its optimization that need to be addressed. The development of effective models remains an open area of research. This review has highlighted the potential of MPC to revolutionize power control and opens the way for further study and innovation.

2.3 Sliding Mode Control

The fundamental premise of SMC lies in the formulation of a control action u ensuring the states of a given system to converge on the sliding surface $s(x) = 0$ in a finite time period and remain there [23]. As illustrated in Figure 7, this controller architecture exhibits stability, even amidst disturbances, depicted by the block $1/(us+1)^2$ in the figure. Nonetheless, the control action's discontinuity, expressed as $sign(s)$, instigates a cyclic behaviour in the output, referred to as chattering. The validation of stability in this control mode utilises Lyapunov methods [24, 25].
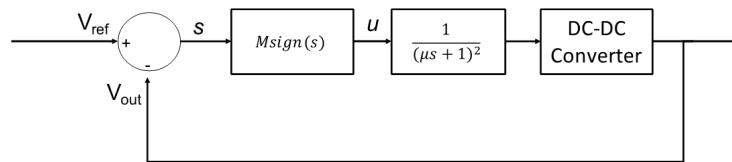

Figure 7. Block diagram of conventional SMC control

To operationalise SMC, it is mandatory to have a model of the converter in a state-space form. Subsequently, the sliding surface and control action, which adhere to Lyapunov stability methods, are defined. The load current x_1 and its derivative x_2 are the state variables for a bidirectional (DAB) [26]. The control action gets defined as per Eq (3). Eq. (4) presents the control action for a boost converter within a hybrid energy storage system [27].

$$u = \frac{\ddot{x}_1^{ref} + \alpha x_1 + \gamma x_2 + \lambda y_2 + KS + n\,\text{sign}(S)}{\beta} \tag{3}$$

$$u = 1 - \frac{\hat{V}_{in} - \alpha_1 L\widehat{x_1}}{\hat{x}_2} + KD_0^{-\lambda}(\text{sign}(S)) \qquad (4)$$

Chattering, an effect attributable to the $sign(S)$ ffunction, becomes evident from Eq. (3) and Eq. (4). To circumvent this, a continuous control action is proposed for an interleaved boost converter to attain robust control against unmodelled dynamics and disturbances [28] . SMC presents the additional benefit of controlling nonlinear systems without necessitating complex linearization procedures, as exemplified by the control of a boost converter for a PV panel with a single power switch, high voltage gain, and a state-space system that doesn't require linearization [29].

2.4 Other Approaches

Revisions to the control methodologies of bidirectional DC-DC converters have been proposed, with the aim of optimizing energy storage systems [30–36]. An innovative method, Time Delay Control, has been presented for use within this converter type [30]. This approach leverages delayed information to account for disturbances and unmodeled system dynamics. The control action equation for boost mode is presented as follows:

$$u(t) = \frac{V_{bus}(t) - L\hat{i}_L(t - T) + V_{bus}[u(t - T) - 1] - LK\left[V_{bus,ref} - V_{bus}(t)\right]}{V_{bus}(t)} \qquad (5)$$

where, T is the delayed time interval.

This method demonstrates superior performance in comparison to conventional PI control, offering reduced transient times and lower voltage overshoots.

A distinct control approach using general-proportional-integral (GPI) for a buck converter was proposed in another study [31]. Compared to PID, this approach's control action integrates an element to account for the unknown initial rate of change of the output variable v_0, facilitating consideration of external disturbances. The control action is illustrated in Eq. (6) as follows:

$$u_{av} = \frac{LC}{E}v + \frac{L}{ER}\dot{F} + \frac{1}{E}F \qquad (6)$$

In the realm of DC-DC converter control, a multitude of diverse methodologies has been suggested. A notable example is the reference signal tracking (RST) polynomial control used for hybrid energy storage in an electric boat [32]. A three-phase interleaved boost converter and a bidirectional boost-buck interface, which serve to supply energy from a fuel cell and a battery to the propulsion motor, incorporate this approach. RST is generally considered to be more robust than PID, although no direct comparison is provided in the study. Furthermore, frequency discrimination is utilized to guide the high transient energy demand towards the battery.

Some research reported the use of a three-level CLLC resonant converter for a microgrid, employing pulse frequency modulation to vary the switching frequency from 31 kHz to 70 kHz [33]. To regulate the gate signals, both current control and voltage control modes are implemented. A Multi-Step current control was employed for a bidirectional converter in an EV charging application [34]. The strategy of stochastic generation of the duty cycle for a boost converter in CMC was executed and compared against PID [35].

Lastly, a DC-DC buck converter designed for wearable devices utilized adaptive voltage scaling (AVS) with inner and outer control loops [36]. This technique facilitated reduced transient times through the employment of a coarse voltage preset block. Overall, these assorted methods illustrate the extensive research conducted to optimize the performance of bidirectional DC-DC converters in various applications. The merits and limitations of these methodologies require further exploration to ascertain their suitability in real-world applications.

3 Artificial Intelligence Control

3.1 Neural Networks Control

Neural networks represent a compelling approach to system modelling in industrial contexts, addressing the complexity and multifaceted nature of these processes. The process of identifying a plant model often outweighs its benefit due to high costs. However, Neural Networks provide a solution that can be easily applied, based on existing data, and is applicable across different scenarios [17]. A popular variant of this solution is the two-layer feedforward neural network (as shown in Figure 8), which employs a widely-used training method: backpropagation. This method involves the minimization of a cost function to estimate the weight values, w_l^p [37].

Even as more complex neural network architectures have emerged, the foundational structure illustrated in Figure 8 remains a prevalent choice for the control of DC-DC converters. Convincing evidence has been presented that a neural network equipped with a single hidden layer and sufficient neurons can accurately model any nonlinear function [22]. A specific implementation of this setup, featuring a three-input neural network with six neurons in the hidden layer and a single-neuron output, has been successfully applied in modelling a single-input/double-output
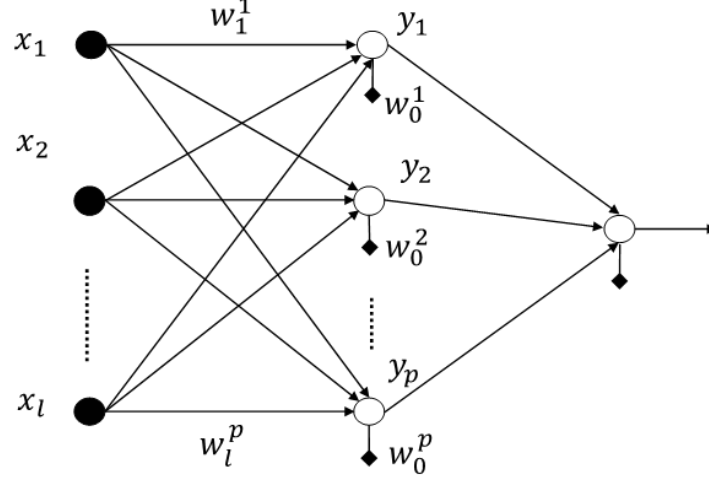
Figure 8. Two-layer feedforward neural network

buck converter [38, 39]. The network operates by predicting future output voltage values, which are subsequently combined with a PID to estimate the control action. When compared to a standard model, this PID-NN approach demonstrated a reduced overshoot and shorter transient times.

Further diversification of neural networks for control purposes can be observed in their arrangement for advanced control methods. For instance, a neural network was trained to estimate the duty cycle for a boost converter, with the estimated duty cycle then fed into another network, trained to predict the output of the converter [40]. The output was subsequently fed to yet another network, termed the 'critic network'. Feedback from this critic network was then employed to adjust the weights of the initial network. Comparative analysis against PI showed that this approach offers a faster transient response.

Challenges arise when attempting to manage the high switching frequencies produced by Wide Bandgap (WGB) devices. These devices necessitate the computation of complex control procedures in a minimal timeframe. To address this issue, neural networks have been implemented for a buck converter operating at a 1 MHz switching frequency [21, 22]. The control laws for explicit MPC, simulated offline, were utilized to train a neural network featuring four inputs and a hidden layer composed of eight neurons. Compared to PID, SMC, and CMC, this approach demonstrated faster settling times [22].

Equally, the MPC principle was adopted in an approach employing a neural network with four inputs and one hidden layer containing eight neurons, designed to model the nonlinear behavior of a converter [21]. The control action is encapsulated in Eq. (7),

$$H = \text{ReLU}\left[W_{IH}X(k) + B_H\right] \tag{7}$$

$$u_{RL}(k+1) = \text{ReLU}\left[W_{IH}X(k) + B_H\right]$$

where, H is the output from the hidden layer, $X(k) = [V_{in}(k), i_L(k), v_0(k), i_0(k)], W_{IH}, B_H, W_{HO}, B$ represent the weight matrices, with ReLU as the activation function. The reward function, optimized to update the network's weights and account for parameter deviations, is notably absent from other comparative approaches. This approach was practically validated with an FPGA. Nonetheless, a comparison with alternative approaches has not been provided. Figure 9 presents a block diagram of the proposed method. The inputs for the NN consist of the sampled variables $X(k)$, which are used to determine the duty cycle control action.

Further developments in the field have leveraged the DAB, an increasingly popular isolated DC-DC topology. In controlling DAB, three variables can be manipulated: the duty cycles of the input and output bridges, and the phase difference between them. When only the phase shift is manipulated, the duty cycles maintain a fixed value, and a PI control determines the amount of phase shift. This is referred to as conventional phase-shift control (CPSC). When the duty cycles are also manipulated, a look-up table houses the combinations of phase-shift and duty cycles that deliver the necessary output power, termed double phase-shift (DPSC) if one duty cycle is involved, and triple phase-shift (TPSC) if both duty cycles are engaged. A novel approach involved the use of two cascaded PID blocks to regulate the amount of phase shift, coupled with a neural network to replace the look-up table for TPSC [41]. The aim of utilizing neural networks in this scenario was to reduce resource requirements for hardware implementation.

In another DAB topology study, a combination of neural networks, PI, particle swarm optimization (PSO), and a fuzzy inference system (FIS) were employed for TPSC [42]. The neural network output the power loss from various
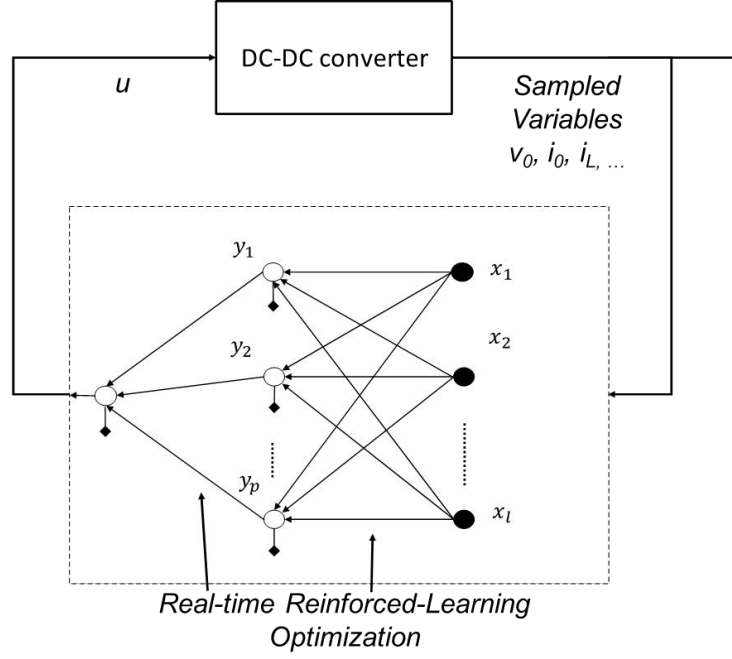
Figure 9. Neural network with RL [21]

combinations of output power, output voltage, and duty cycles. Two hidden layers containing 256 and 32 neurons, with ReLU activation functions, were used. The output from the neural network was then used by the PSO algorithm to estimate the optimal duty cycles.

In conclusion, these advancements in neural network applications for control scenarios showcase the versatility and robustness of these networks in addressing complex and intricate industrial processes. As further research continues, the performance and efficiency of these networks will likely improve, leading to more accurate and responsive systems across various application scenarios.

3.2 Fuzzy Logic Control

Fuzzy Logic Control (FLC) encapsulates a computational technique wherein the output acknowledges the inherent vagueness prevalent in real-world scenarios. Diverging from binary responses, FLC operates within the continuum of [0,1]. Figure 11 illustrates the architecture of the Type-2 Fuzzy Logic Control (T2-FLC), which envelops the Type-1 FLC (T1-FLC) as a unique case. It is observed that T1-FLC disregards uncertainties, assuming one-dimensional input membership functions [34, 43]. Notable components of the FLC procedure include a fuzzifier, an inference engine, a rules set, and output processing. Specifically, the output processing for T2-FLC incorporates a type reducer and a defuzzifier. The key advantage lies in bypassing the intricate process of model derivation; knowledge of the system manifests as a rules set correlating the input with the intended control action.

The DAB topology, popular in contemporary discussions, witnessed the implementation of T1-FLC, with comparisons drawn to SMC [26]. It was demonstrated that current control via FLC resulted in finer power regulation than SMC. Interestingly, the current measurement alone sufficed for the control design, eliminating the need for a converter model. However, this model-less approach was found to be potentially unstable, necessitating Lyapunov stability analysis for estimating defuzzification parameters. Conventionally, the error and the change in error are employed as input signals for the FLC, a strategy evident in Figure 10.

The applicability of T1-FLC extends to two bidirectional converters in electric vehicles (EVs). One manages the power flow for motor propulsion [44], while the other oversees a hybrid energy storage system with dual inputs [45]. Despite distinct circuit topologies and functionalities, both utilized seven triangular input membership functions each for error and change in error. This fact underscores the adaptability of FLC to diverse systems with minimal design modifications.

An insightful comparison was conducted between T1 and T2 Fuzzy-PI for a boost converter [46]. The control action, as indicated in Eq. (8), entails the control output from the FLC, denoted as $\widehat{u}_1$, along with the proportional G_1 and integral gains G_2 of the PI control. The comparison scheme is outlined in Figure 11. Remarkably, T2-FLC showcased faster settling times than T1-FLC. When transitioning from T1 to T2 FLC, the uncertainty in the membership function was manually specified. Later, PSO and Invasive weed optimization (IWO) were introduced for determining the optimal uncertainty regions for T2 FLC. The addition of these optimization methods led to an
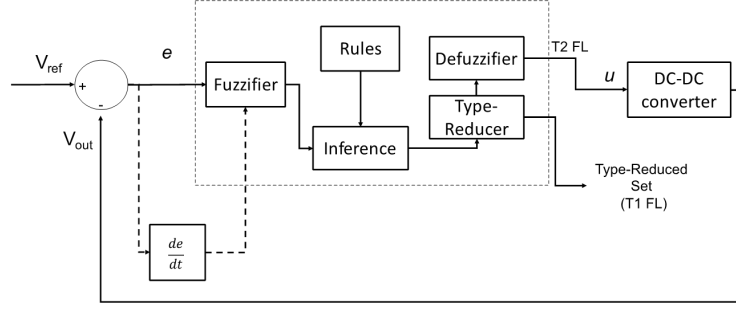
Figure 10. Block diagram of type-2 Fuzzy Logic control

enhancement in settling times, relative to the fuzzy-PI without optimization [47].

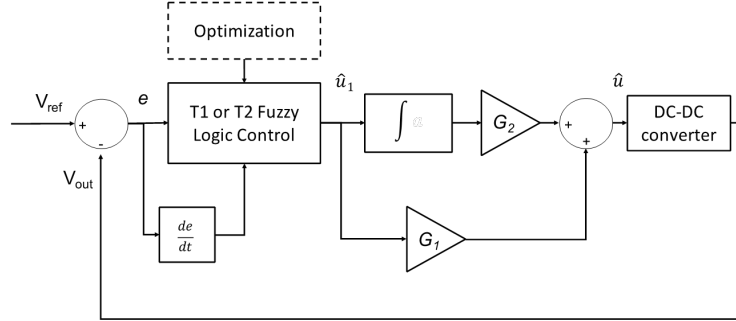$$\hat{u} = G_1\hat{u}_1 + G_2 \int \hat{u}_1 d\tau \tag{8}$$

Figure 11. Fuzzy-PID with PSO and IWO [47]

In conclusion, Fuzzy Logic Control presents a promising technique for managing inherent uncertainties in complex systems, thereby creating smoother and more efficient controls. The transition from T1 to T2 FLC indicates a trend towards dealing with more complex situations where uncertainties are not always one-dimensional and need to be better represented in the control architecture. The various applications of T1-FLC and T2-FLC, their comparisons, and the role of optimization techniques further enrich our understanding of FLC as an emerging control methodology. However, it is imperative to delve deeper into stability issues and optimal uncertainty determination for the wider application and efficacy of these control methods.

4 Discussion

In the preceding sections, numerous control techniques have been scrutinized, with little regard for the circuit topologies involved. However, it's crucial to note that the effectiveness of a control approach is intrinsically tied to the specific converter type employed. Conventional control techniques, for instance, yield divergent models and, consequently, control responses based on the topology applied. Hence, this part of the discussion groups control methods in accordance with their respective circuit topologies.

Five principal topology categories have been delineated: buck, boost, bidirectional, DAB, and multi-input/output. The findings are systematically displayed in Tables 1 to 5. The basic buck configuration represents the first topology and is depicted in subgraph a) of Figure 12. It was noted that PID was the most commonly implemented control method, often used in a comparative capacity to validate the performance of the primary methods, as indicated in Table 1. Notably, this topology is characterized by exceptionally high switching frequencies at low voltages, typically validated experimentally with FPGAs.

The elementary boost topology, portrayed in subgraph b) of Figure 12, is the subject of Table 2. Contrary to the buck configuration, this topology is marked by lower switching frequencies at low operational voltages and is predominantly explored through simulations. Similar to the previous case, PID emerges as the most frequently employed control method, acting either as a benchmark for comparison or in conjunction with advanced techniques. It's noteworthy that FL and SMC are more prevalent in this topology. A trio of boost topologies were discovered, incorporating interleaving and switched capacitor, which serve to mitigate current ripples and voltage stress in the components. SMC and RST are preferentially applied in these configurations (Table 2).

Table 1. Control algorithms for buck topologies

Ref[2]	Switch Freq.	Control	Vi/Vo	Hardware[3]
	kHz		VDC	
[39]	–	NN, PID	30/10	Simulation
[21]	1000	NN, RL	48/24	FPGA
[31]	48.8	GPI PID	24/18	FPGA
[18]	100	LPV MPC PID	12/5	FPGA
[36]	2000	P-AVS	3.3/07	CMOS*
[22]	1000	MPC,NN	60/30	FPGA
[2]*	> 400	PI	160/24	μ Controller**

1. NN – Neural network, PID – Proportional Integral Derivative, RL – Reinforcement Learning, GPI – General Proportional Integral, LPV – Linear Parameter Varying, MPC – Model Predictive Control, P-AVS – Preset Adaptive Voltage Scaling 2. Elementary buck topology, *2-phase interleaved buck with LLC isolation 3. General Purpose application, *wearables, **railway.
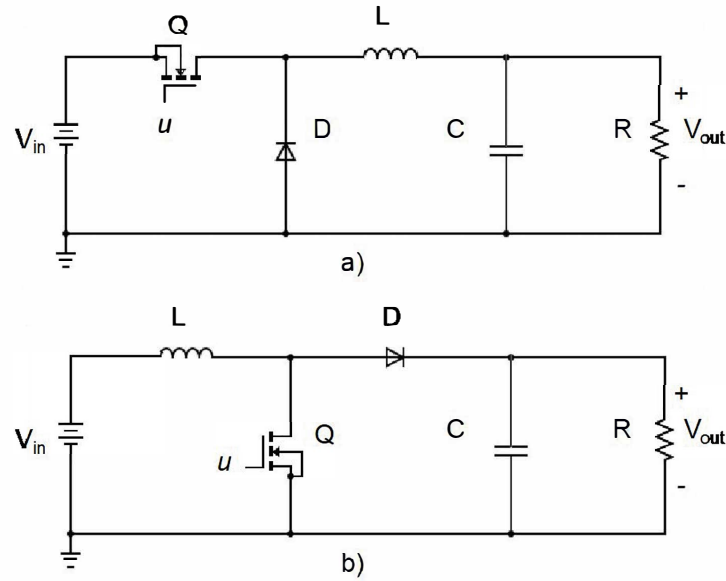
Figure 12. a) buck (Table 1) and b) boost (Table 2) topologies

Table 2. Control algorithms for boost topologies

Ref[2]	Switch Freq.	Control	Vi/Vo	Hardware / Simulation[3]
	kHz		VDC	
[39]	–	NN, PID	25/28	Simulation
[40]	20	DHP-NN , PI	$60/200 - 700$	Simulation
[35]	1000	PI-SDC	1/1.67	Simulation
[46]	5	T1& T2 FL-PID	15/38	Simulation
[27]	–	AFSMC, SMC	25/50	Simulation
[14]	30	DICS-PI	38/48	Simulation *
[47]	5	TI & T2 FL-PID (IWO \PSO)	15/37.5	Simulation
[28]*	100	CfNSFT-SMC	24/48	dSPACE
[32]*	10	RST	70/105	dSPACE*
[29]**	50	SMC	24/240	FPGA*8

1. NN – Neural network, PID – Proportional Integral Derivative, DHP – Dual heuristic Programming, SDC – Stochastic Duty Cycle, FL – Fuzzy Logic, SMC –Sliding Mode Control, AFSMC – Fractional SMC, DICS – Improved Startup Dynamics, IWO –Invasive Weed Optimization, PSO – Particle Swarm Optimization, CfNSFT – Chatter free non-singular fast terminal, RST – Reference Signal Tracking 2. Elementary boost topology, *Interleaved, ** Switched Capacitor

3. General Purpose application, *Electric Vehicles, **Photovoltaic Panel.

The elementary bidirectional topology, depicted in subgraphs a) and b) of Figure 13, corresponds to the buck-boost mode and its symmetrical counterpart, the boost-buck, respectively. The switching frequencies are maintained

low as in the case of the boost topology, but a rise in the operating voltages is evident. As observed in previous instances, PID is the control method of choice, with the frequency of SMC, MPC, FL, and NN dropping when compared to the earlier topologies. For these circuits, interleaving and multilevel configurations are also present, predominantly featuring PID control (Table 3).
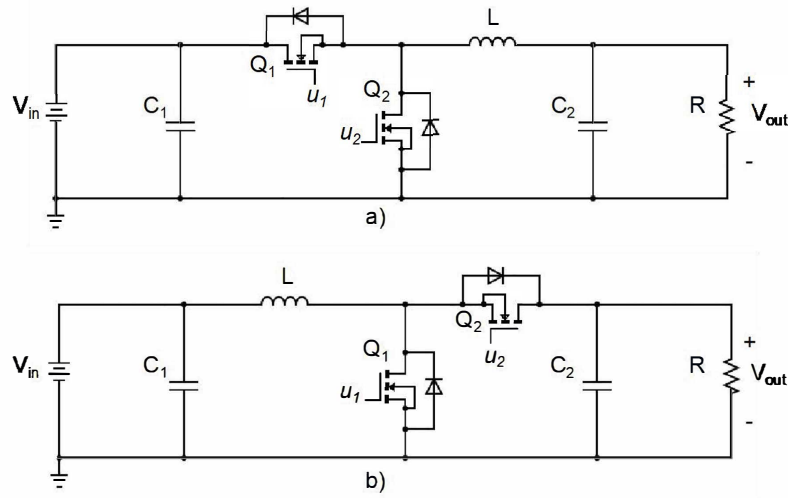

Figure 13. Bidirectional a) buck-boost and b) boost-buck

Table 3. Control algorithms bidirectional topologies

Ref[2]	Switch Freq. kHz	Control	Vi/Vo VDC	Hardware / Simulation[3]
[39]	–	NN, PID	12/5	Simulation*
[34]	10	MSCC-PI	750/360	Simulation
[16]	20	PI	450/280	FPGA
[22]	1000	MPC NN	60/24	FPGA*
[7]	10	PI	300/120	Simulation
[33]	70	PFM	750/200	Simulation
[30]*	30	TDC, PI	18/30	NI-LabView
[44]*	200	FL	378/500	Simulation
[32]*	10	RST	60/105	dSPACE
[9]*	50	PI-DB	40/200	μController

1. NN – Neural network, PID – Proportional Integral Derivative, MSCC – Multiple Step Constant Current, MPC – Model Predictive Control, MSCC - , PFM – Pulse Frequency Modulation, TDC – Time Delay Control, FL – Fuzzy Logic, RST – Reference Signal Tracking, DB – Dead Beat

2. Buck-boost, *boost-buck.

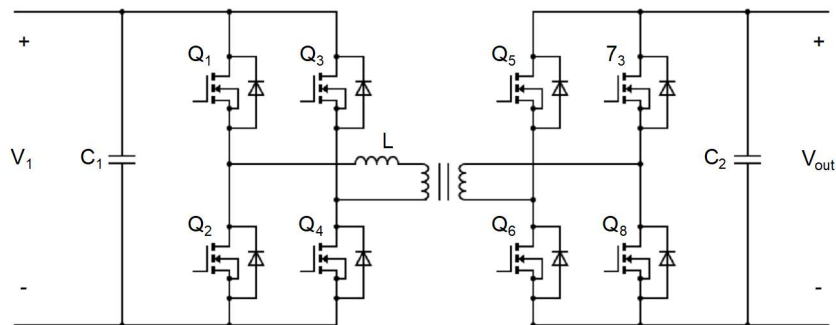3. Electric Vehicles applications, *General Purpose application.

Figure 14. Dual-Active-Bridge (DAB) topology

Table 4. Control Algorithms for DAB topologies

Ref	Switch Freq.	Control	Vi/Vo	Hardware / Simulation[3]
	kHz		VDC	
[26]	100	FL, SMC	270/28	Simulation*
[11]	2	PI	1100/	FPGA**
[41]	50	LR-KNN-RF-NN, TPSC-PI	400/	Simulation
[42]	20	NN-PSO-FI, TPSC	200/160	dSpace
[19]	100	MPC, PI	270/28	Simulation +

1. NN – Neural network, PI – Proportional Integral, MPC – Model Predictive Control, FL – Fuzzy Logic, LN – Linear Regression, KNN – k-neareast neighbor, RF – Random Forest, TPSC – triple phase shift control, PSO –Particle swarm optimization.

3. General purpose, *battery charging, **grid, +aircraft

A dedicated category was established for the DAB topology, showcased in Figure 14 and summarized in Table 4. The control of power flow is accomplished through manipulating the phase-shift between the input and output bridges. As alluded to earlier, the duty cycles can be kept constant for standard PS or adjusted for double or triple PS to enhance the efficiency of converter operation. In a similar vein, PID remains the method of choice for comparative analysis. However, a trend towards more predominant use of AI control methods as the principal control technique is discernible. This topology is also characterized by elevated operating voltages at medium-low switching frequencies (Table 4).

Table 5. Control for multiple input/output topologies

Ref	Switch Freq.	Control	Vi/Vo	Hardware / Simulation[3]
[3]	20	PI	36/125	Simulation
[4]	10	PI	16/28	dSpace
[5]	20	PI	12/72	Simulation
[6]	10	PI	12/58	dSpace
[8]	50	PI	48/12, 5	Simulation
[10]	350	PI	$50 - 500/750$	Simulation
[38]	200	PI NN	36/5	Simulation*
[45]	–	PI FL	100/40	Simulation
[12]	20	PI	12/50	dSpace**
[20]	250	MPC	12/4	dSpace

1. NN – Neural network, PID – Proportional Integral Derivative, MPC – Model Predictive Control, FL – Fuzzy Logic,

3. Electric Vehicle applications, *general purpose **microgrids

The final category encompasses the multi-input/output converters, whose findings are compiled in Table 5. This section incorporates a diverse range of configurations, such as interleaving, multi-level with double or triple ports. Operating voltages are predominantly low, coupled with medium-low switching frequencies. Interestingly, PI is the dominant control method in this context. There appears to be an inclination to apply complex or advanced control methods to the more fundamental circuit topologies, like buck and boost. However, as the complexity of the topologies escalates, a simple PI control block can be orchestrated in parallel and cascade setups, demonstrating its flexibility (Table 5).

The assessment of advantages and disadvantages associated with each control methodology was carried out via simulations, based on the buck and boost topologies as depicted in Figure 12. Components' values were aligned with those reported in the study [22], with a switching frequency set at 1 MHz. This high switching frequency aimed to increase the power density of the converter through the reduction of the passive components' size, although it presented additional control method challenges due to the diminished time available for the calculation of the required control action.

Utilized for implementation on the elementary buck and boost topologies were the basic algorithms from the study [48], which comprised PID, MPC, NN, and FL. For PID, the small-signal transfer functions were utilized for tuning as per [49], with outcomes depicted in Figures 15 and 16, for the buck and boost converters, respectively. A step change in reference voltage around the operational point D=0.5 was applied to both converters.

Notable in the results was the role of PID in decreasing the settling time of the buck converter, albeit with a slight increase in peak overshoot (Figure 15). In the case of the boost converter, PID eliminated the undershoot completely, though it led to an extended settling time (Figure 16). The right half plane zero in the boost converter's transfer function added complexity to its control [35, 49]. PID control acted as a benchmark for comparison with the subsequent algorithms.

Elementary PID configuration from Figure 3 was used without the need for additional complex configurations. This strategy was to provide an overview of the fundamental design process. Then, the other control methods were also implemented in the elementary configurations for a fair comparison. The averaged state-space model, extensively used for converter control design [18, 22, 27, 46, 47, 49], was employed for the design of the following controls.
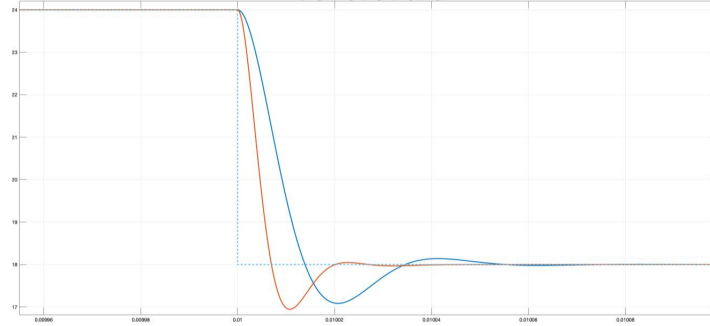

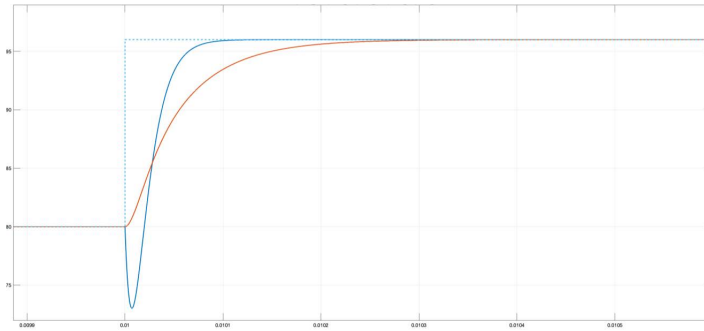**Figure 15.** Open-loop buck converter (solid blue) vs. PID close-loop control (solid red)

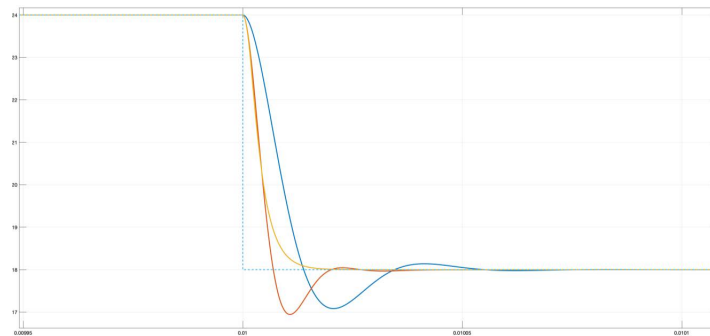**Figure 16.** Open-loop boost converter (solid blue) vs. PID close-loop control (solid red)

Figure 17. Open-loop buck converter (solid blue) vs. PI (solid red) and MPC (solid orange)

The second methodology was the MPC. Figures 17 and 18 respectively display the step response for the buck and boost scenarios. In the buck case, the output voltage reached the reference voltage more swiftly than with PID control, without overshooting (Figure 17). Conversely, in the boost scenario, the output voltage merely remained in proximity to the desired output voltage (Figure 18).

Following this, a Neural Network (NN) was implemented, which had two inputs, a single hidden layer with thirteen neurons, and one output. Training was conducted with data obtained from the MPC model. Figure 19 illustrates the output response for the buck case, and Figure 20 for the boost case. The NN attained the reference value but with an increased overshoot and settling time. The boost case indicated a faster response than PID, although it never fully converged to the reference value, as was expected from the MPC training data. The NN method's advantage lies in its capacity to learn from input data without necessitating a system model. However, tuning it is
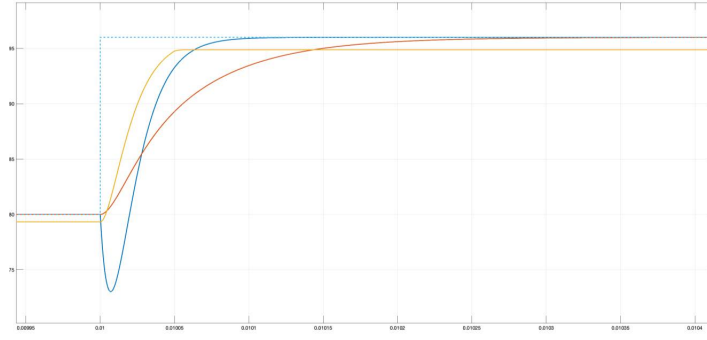
Figure 18. Open-loop boost converter (solid blue) vs. PI (solid red) and MPC (solid orange)

more complex than tuning PID since the impact of changes in the internal NN weights on the output signal is difficult to assess. Moreover, the quality of the training data directly influences the NN's output.
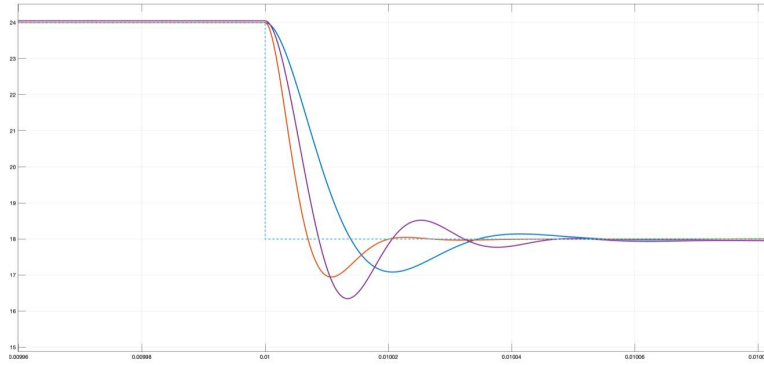

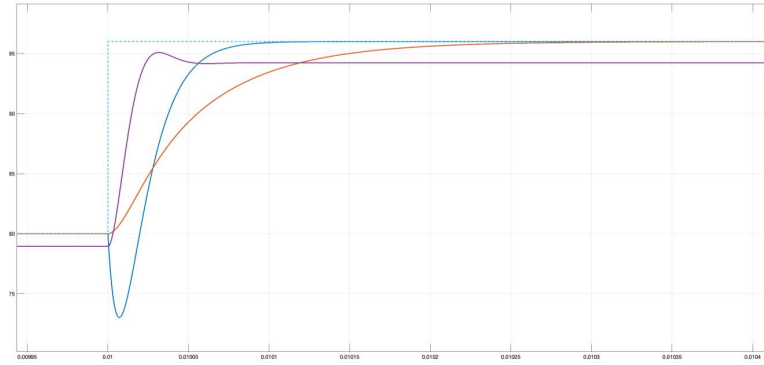**Figure 19.** Open-loop buck converter (solid blue) vs. PI (solid red) and NN (solid purple)

Figure 20. Open-loop boost converter (solid blue) vs. PI (solid red) and NN (solid purple)

Finally, a Fuzzy Logic (FL) controller was implemented, comprising a single input and output with three inference rules. The output for the buck and boost cases is presented in Figures 21 and 22, respectively. For the buck case, a larger ripple and settling time were observed, compared to PID, and the output failed to converge, remaining close to the desired value. The boost case output was faster than PID, but it also failed to reach the setpoint, remaining only in proximity to it. The advantage of this method is that it can be designed without the necessity for complex derivations of a plant model. However, running times increased compared to the other models, which could pose an issue for real-time implementation.

Tables 6 and 7 summarize the performance of all implemented methods by measuring the rise time T_r, peak time T_p, maximum overshoot M_p, settling time T_s, the final output voltage V_{out}, and the difference between the final output voltage and the reference voltage ϵ. A value of 2% of the reference voltage was selected for the settling time [1]. Even though MPC, NN, and FL failed to fully converge, they all managed to reach within 2% of the reference value. The shortest rise time was achieved by the MPC in the buck case without overshoot. For the boost
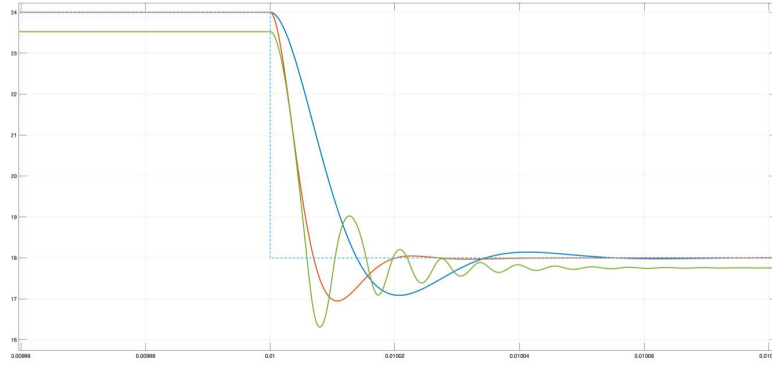
Figure 21. Open-loop buck converter (solid blue) vs. PI (solid red) and FL (solid green)
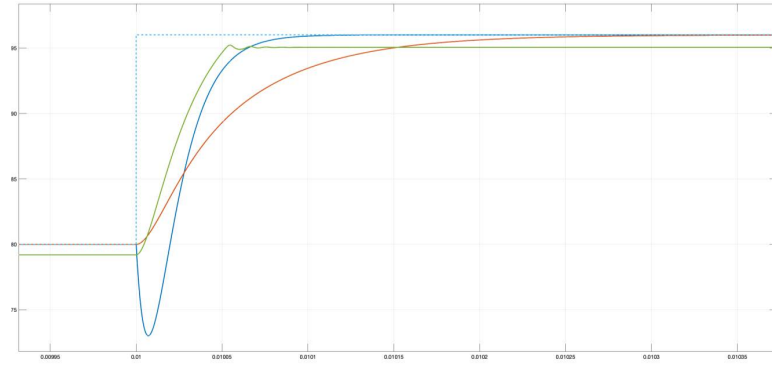

Figure 22. Open-loop boost converter (solid blue) vs. PI (solid red) and FL (solid green)

Table 6. Performance comparison for Buck control

Control	T_r (s)[1]	T_p (s)[2]	M_p (V)	T_s (s)[2]	V_{out} (V)	ϵ
PID	6.73	1.06	5.8	1.62	18	0
MPC	NA	NA	NA	0.972	18	0
NN	8.68	1.34	9.2	2.84	17.96	0.04
FL	5.89	0.795	9.38	3.68	17.75	0.25

1. E-6, 2. E-5

Table 7. Performance comparison for Boost control

Control	T_r (s)[1]	T_p (s)[1]	M_p (V)	T_s (s)[2]	V_{out} (V)	ϵ
PID	3.74	3.74	0	37.4	95.99	0.01
MPC	NA	NA	0	5.45	94.87	1.13
NN	NA	NA	0	5.95	94.17	1.83
FL	NA	NA	0	5.22	95.05	0.95

1. E-4, 2. E-5

case, the shortest rise time was obtained with FL, although the smallest ϵ was observed with PID.

5 Conclusions

The extensive exploration conducted herein provides an exhaustive review of control methodologies employed in DC-DC power converters. The proposed taxonomy categorizes the control algorithms into two distinct groups: Traditional Control Methods, encompassing PID, MPC, SMC, and others, and Artificial Intelligence-based Methods, including Neural Networks (NN), Fuzzy Logic (FL), among others.

Additionally, these control methods have been further dissected based on their applicability to various circuit topologies, prominently buck, boost, bidirectional buck-boost, Dual Active Bridge (DAB), and multi-input/output. Crucial simulations were carried out for elementary buck and boost topologies using four fundamental, commercially

available control algorithms to facilitate the comparative analysis of each control methodology.

The PID control method remains the most prevalent due to its relatively uncomplicated implementation process. A thorough design and stability analysis using frequency or root locus methods is feasible once the converter is linearized around a chosen operating point. However, deviations from this operating point may lead to potential degradation of the control algorithm's performance.

In terms of settling times and zero voltage overshoot, the Model Predictive Control (MPC) exhibited superior performance compared to PID. The effectiveness of the Neural Network, on the other hand, was found to be heavily reliant on the training data input. Unlike other methods requiring a single input, the NN necessitated two inputs to initiate a proper control action.

Fuzzy Logic proved its competency by controlling both topologies with a single input/output and a simple three-rule inference configuration. Nevertheless, the processing speed of FL was noticeably slower, posing a challenge for real-time implementation at high switching frequencies.

A distinctive advantage of AI control methodologies over traditional methods lies in their ability to function without the necessity of a precise linear model of the system. However, this comes with the caveat of needing vast quantities of data for NN training. Moreover, the process of determining which variables to use for training remains empirical, and thus, there is room for improvement in this regard.

To enhance the effectiveness and efficiency of these control methods, future studies could focus on optimizing the selection process for training variables and enhancing the processing speed for methods such as Fuzzy Logic, thereby making them more suitable for real-time applications.

Data Availability

The data used to support the findings of this study are available from the corresponding author upon request.

Conflicts of Interest

The authors declare that they have no conflicts of interest.

References

[1] K. Ogata, *Modern Control Engineering*. Prentice Hall, 2010.

[2] M. Fu, C. Fei, Y. Yang, Q. Li, and F. C. Lee, "A GaN-based DC-DC module for railway applications: Design consideration and high-frequency digital control," *IEEE Trans. Ind. Electron.*, vol. 67, no. 2, pp. 1638–1647, 2020. https://doi.org/10.1109/TIE.2019.2896279

[3] A. Ganjavi, H. Ghoreishy, A. Ahmad, and Z. Zhagn, "A three-level three-port bidirectional DC-DC converter," in *Proceedings - 2018 IEEE International Power Electronics and Application Conference and Exposition, PEAC 2018*. Shenzhen, China: IEEE, 2018, pp. 1–4. https://doi.org/10.1109/PEAC.2018.8590338

[4] P. Bhattacharyya, A. Banerjee, S. Sen, S. K. Giri, and S. Sadhukhan, "A modified semi-active topology for battery-ultracapacitor hybrid energy storage system for EV applications," in *2020 IEEE Int. Conf. Power Electron. Smart Grid Renew. Energy (PESGRE)*. Cochin, India: IEEE, 2020, pp. 1–6. https://doi.org/10.1109/PESGRE45664.2020.9070531

[5] B. B. T. Shekin and K. Biju, "A multi-input switched capacitor bidirectional DC-DC converter with triple closed loop control for electric vehicle application," in *2021 IEEE Int. Power Renew. Energy Conf. (IPRECON)*. Kollam, India: IEEE, 2021, pp. 1–6. https://doi.org/10.1109/IPRECON52453.2021.9640824

[6] K. Suresh, C. Bharatiraja, N. Chellammal, M. Tariq, R. K. Chakrabortty, M. J. Ryan, and B. Alamri, "A multifunctional non-isolated dual input-dual output converter for electric vehicle applications," *IEEE Access*, vol. 9, pp. 64 445–64 460, 2021. https://doi.org/10.1109/ACCESS.2021.3074581

[7] O. Alkul and S. Demirbas, "A novel high frequency-link bidirectional DC-DC converter for electric vehicle applications," in *2019 2nd International Conference on Smart Grid and Renewable Energy (SGRE)*. Doha, Qatar, IEEE, 2019, pp. 1–6. https://doi.org/10.1109/SGRE46976.2019.9020693

[8] M. Ramesh, B. Mallikarjuna, and T. Rajasekar, "A novel investigation on single-input three-output DC-DC buck converter for electrical vehicles," in *2021 7th International Conference on Electrical Energy Systems (ICEES)*. Chennai, India: IEEE, 2021, pp. 141–146. https://doi.org/10.1109/ICEES51510.2021.9383635

[9] H. Heydari-doostabad and T. O'Donnell, "A wide-range high-voltage-gain bidirectional DC–DC converter for V2G and G2V hybrid EV charger," *IEEE Trans. Ind. Electron.*, vol. 69, no. 5, pp. 4718–4729, 2022. https://doi.org/10.1109/TIE.2021.3084181

[10] G. R. Chandra Mouli, J. Schijffelen, M. Van Den Heuvel, M. Kardolus, and P. Bauer, "A 10 kW solar-powered bidirectional EV charger compatible with chademo and COMBO," *IEEE Trans. Power Electron.*, vol. 34, no. 2, pp. 1082–1098, 2019. https://doi.org/10.1109/TPEL.2018.2829211

[11] A. J. Watson, P. W. Wheeler, and J. C. Clare, "Field programmable gate array based control of dual active bridge DC/DC converter for the UNIFLEX-PM project," in *Proc. 2011 14th Eur. Conf. Power Electron. Appl. EPE 2011*. Birmingham, UK: IEEE, 2011, pp. 1–10. https://doi.org/10.1109/EPE.2011.6020479

[12] T. Jiao, X. Zhang, B. Wang, G. Cui, and W. Ma, "A multiple-port three-level DC/DC converter for HESS with power sharing in DC microgrids," *Chinese J. Electron.*, vol. 30, no. 3, pp. 570–583, 2021. https://doi.org/10.1049/cje.2021.04.011

[13] M. Z. Hossain, N. A. Rahim, and J. Selvaraj, "Recent progress and development on power DC-DC converter topology, control, design and applications: A review," *Renew. Sustain. Energy Rev.*, vol. 81, pp. 205–230, 2018. https://doi.org/10.1016/j.rser.2017.07.017

[14] A. Campanini, M. Simonazzi, L. Sandrolini, C. Rossi, and M. Bosi, "Fast dynamic control for a boost DC/DC converter in hybrid-electric powertrain with PEM fuel cell and battery pack," *Electr. Eng.*, vol. 105, pp. 1585–1595, 2023. https://doi.org/10.1007/s00202-023-01761-2

[15] M. Lešo, J. Žilková, M. Biroš, and P. Talian, "Survey of control methods for DC-DC converters," *Acta Electrotech. Inform.*, vol. 18, no. 3, pp. 41–46, 2018. https://doi.org/10.15546/aeei-2018-0024

[16] A. Ali, N. Faisal, Z. Zia, I. Makda, and A. Usman, "Rapid prototyping of bidirectional DC-DC converter control using FPGA for electric vehicle charging applications," in *2022 IEEE 13th International Symposium on Power Electronics for Distributed Generation Systems (PEDG)*. Kiel, Germany: IEEE, 2022, pp. 1–6. https://doi.org/10.1109/PEDG54999.2022.9923288

[17] M. A. Henson and D. E. Seborg, *Nonlinear Process Control*. Prentice Hall PTR, 1997.

[18] Z. Liu, L. Xie, A. Bemporad, and S. Lu, "Fast linear parameter varying model predictive control of buck DC-DC converters based on FPGA," *IEEE Access*, vol. 6, pp. 52 434–52 446, 2018. https://doi.org/10.1109/ACCESS.2018.2869043

[19] Y. Zhu, Z. Wang, T. Yang, T. Dragicevic, S. Bozhko, and P. Wheeler, "Model predictive control for DC offset suppression of dual active bridge converter for more-electric aircraft applications," in *IEEE Int. Symp. Ind. Electron.* Kyoto, Japan: IEEE, 2021, pp. 0–5. https://doi.org/10.1109/ISIE45552.2021.9576199

[20] K. Shi, T. Bui, and J. Marco, "Optimal control of bidirectional active clamp forward converter with synchronous rectifier based cell-to-external-storage active balancing system," *J. Energy Storage*, vol. 41, p. 102851, 2021. https://doi.org/10.1016/j.est.2021.102851

[21] J. Chen, Y. Chen, and Y. Kang, "A real-time self-learning control for megahertz GaN-based DC-DC converter," in *IEEE Work. Wide Bandgap Power Devices Appl. Asia, WiPDA Asia 2021*, Wuhan, China, 2021, pp. 157–161. https://doi.org/10.1109/WiPDAAsia51810.2021.9656043

[22] J. Chen, Y. Chen, L. Tong, L. Peng, and Y. Kang, "A backpropagation neural network-based explicit model predictive control for DC-DC converters with high switching frequency," *IEEE J. Emerg. Sel. Top. Power Electron.*, vol. 8, no. 3, pp. 2124–2142, 2020. https://doi.org/10.1109/JESTPE.2020.2968475

[23] V. Utkin, A. Poznyak, Y. Orlov, and A. Polyakov, "Conventional and high order sliding mode control," *J. Franklin Inst.*, vol. 357, no. 15, pp. 10 244–10 261, 2020. https://doi.org/10.1016/j.jfranklin.2020.06.018

[24] K. Ogata, *Discrete-Time Control Systems*. Prentice-Hall, Inc., 1995.

[25] L. B. Koppel, *Introduction to Control Theory*. Prentice-Hall, 1968.

[26] S. Talbi, A. M. Mabwe, and A. El Hajjaji, "Control of a bidirectional dual active bridge converter for charge and discharge of a Li-ion battery," in *IECON 2015 - 41st Annu. Conf. IEEE Ind. Electron. Soc.*, Yokohama, Japan, 2015, pp. 849–856. https://doi.org/10.1109/IECON.2015.7392205

[27] J. Wang, D. Xu, H. Zhou, and T. Zhou, "Adaptive fractional order sliding mode control for boost converter in the batterysupercapacitor HESS," *PLoS One*, vol. 13, no. 4, pp. 1–10, 2018. https://doi.org/10.1371/journal.pone.0196501

[28] S. V. Malge, M. G. Ghogare, S. L. Patil, A. S. Deshpande, and S. K. Pandey, "Chatter-free non-singular fast terminal sliding mode control of interleaved boost converter," *IEEE Trans. Circuits Syst. II Express Briefs*, vol. 70, no. 1, pp. 186–190, 2023. https://doi.org/10.1109/TCSII.2022.3201959

[29] Q. Qi, D. Ghaderi, and J. M. Guerrero, "Sliding mode controller-based switched-capacitor-based high DC gain and low voltage stress dc-dc boost converter for photovoltaic applications," *Int. J. Electr. Power Energy Syst.*, vol. 125, p. 106496, 2021. https://doi.org/10.1016/j.ijepes.2020.106496

[30] Y. X. Wang, F. F. Qin, and Y. B. Kim, "Bidirectional DC-DC converter design and implementation for lithium-ion battery application," in *2014 IEEE PES Asia-Pacific Power and Energy Engineering Conference (APPEEC), Kong, China*, 2014, pp. 1–5. https://doi.org/10.1109/APPEEC.2014.7066140

[31] E. W. Zurita-Bustamante, J. Linares-Flores, E. Guzmán-Ramírez, and H. Sira-Ramírez, "A comparison between the GPI and PID controllers for the stabilization of a DC-DC 'buck' converter: A field programmable gate array implementation," *IEEE Trans. Ind. Electron.*, vol. 58, no. 11, pp. 5251–5262, 2011. https://doi.org/10.1109/TIE.2011.2123857

[32] A. Al Amerl, I. Oukkacha, M. B. Camara, and B. Dakyo, "Real-time control strategy of fuel cell and battery system for electric hybrid boat application," *Sustain.*, vol. 13, no. 16, p. 8693, 2021. https://doi.org/10.3390/su13168693

[33] Y. Xuan, X. Yang, W. Chen, T. Liu, and X. Hao, "A novel three-level CLLC resonant DC-DC converter for bidirectional EV charger in DC microgrids," *IEEE Trans. Ind. Electron.*, vol. 68, no. 3, pp. 2334–2344, 2021. https://doi.org/10.1109/TIE.2020.2972446

[34] B. Chelladurai, C. K. Sundarabalan, S. N. Santhanam, and J. M. Guerrero, "Interval type-2 fuzzy logic controlled shunt converter coupled novel high-quality charging scheme for electric vehicles," *IEEE Trans. Ind. Informatics*, vol. 17, no. 9, pp. 6084–6093, 2021. https://doi.org/10.1109/TII.2020.3024071

[35] V. Michal, "Optimal load transient response of the boost DC-DC converter based on stochastic duty-cycle sequence generator," in *2021 31st Int. Conf. Radioelektronika, RADIOELEKTRONIKA 2021*, Brno, Czech Republic, 2021, pp. 1–5. https://doi.org/10.1109/RADIOELEKTRONIKA52220.2021.9420200

[36] P. Luo, D. Wang, and X. Peng, "An adaptive voltage scaling buck converter with preset circuit," *Chinese J. Electron.*, vol. 28, no. 2, pp. 229–236, 2019. https://doi.org/10.1049/cje.2019.01.007

[37] K. Koutroumbas and S. Theodoridis, *Pattern Recognition*. Elsevier Science, 2008.

[38] F. Kurokawa, H. Maruta, T. Mizoguchi, A. Nakamura, and H. Osuga, "A new digital control DC-DC converter with multi-layer neural network predictor," in *2009 International Conference on Machine Learning and Applications*, Miami, FL, USA, 2009, pp. 638–643. https://doi.org/10.1109/ICMLA.2009.106

[39] J. Ramirez-Hernandez, O. U. Juarez-Sandoval, L. Hernandez-Gonzalez, A. Hernandez-Ramirez, and R. S. Olivares-Dominguez, "Voltage control based on a back-propagation artificial neural network algorithm," in *2020 IEEE Int. Autumn Meet. Power, Electron. Comput. ROPEC 2020*, Ixtapa, Mexico, 2020. https://doi.org/10.1109/ROPEC50909.2020.9258699

[40] S. Saadatmand, M. Kavousi, and S. Azizi, "The voltage regulation of boost converters using dual heuristic programming," in *2020 10th Annual Computing and Communication Workshop and Conference (CCWC)*, Las Vegas, NV, USA, 2020, pp. 531–536. https://doi.org/10.1109/CCWC47524.2020.9031276

[41] B. Bohara, A. Karbozov, and H. S. Krishnamoorthy, "Triple phase shift control of dual active bridge converter using machine learning methods," in *2022 IEEE Texas Power and Energy Conference (TPEC)*, College Station, TX, USA, 2022, pp. 1–6. https://doi.org/10.1109/TPEC54980.2022.9750772

[42] F. Lin, X. Zhang, X. Li, C. Sun, W. Cai, and Z. Zhang, "Automatic triple phase-shift modulation for DAB converter with minimized power loss," *IEEE Trans. Ind. Appl.*, vol. 58, no. 3, pp. 3840–3851, 2022. https://doi.org/10.1109/TIA.2021.3136501

[43] O. Castillo, *Type-2 Fuzzy Logic in Intelligent Control Applications*. Berlin, Heidelberg: Springer Berlin Heidelberg, 2012.

[44] N. A. Metin, A. Boyar, and E. Kabalci, "Design and analysis of Bi-directional DC-DC driver for electric vehicles," in *2019 IEEE 1st Glob. Power, Energy Commun. Conf. GPECOM 2019*, Nevsehir, Turkey, 2019, pp. 227–232. https://doi.org/10.1109/GPECOM.2019.8778532

[45] G. Gurjar, D. K. Yadav, and S. Agrawal, "Illustration and control of non-isolated multi-input DC-DC bidirectional converter for electric vehicles using fuzzy logic controller," in *2020 IEEE Int. Conf. Innov. Technol. INOCON 2020*, Bangluru, India, 2020, pp. 2–6. https://doi.org/10.1109/INOCON50539.2020.9298307

[46] A. Bennaoui and S. Saadi, "Type-2 fuzzy logic PID controller and different uncertainties design for boost DC-DC converters," *Electr. Eng.*, vol. 99, no. 1, pp. 203–211, 2017. https://doi.org/10.1007/s00202-016-0412-3

[47] A. Bennaoui, S. Saadi, and A. Ameur, "Invasive weed optimization algorithm for tuning transitioning from type-1 to interval type-2 fuzzy logic controller for boost DC-DC converters," *J. Eur. des Syst. Autom.*, vol. 53, no. 2, pp. 195–202, 2020. https://doi.org/10.18280/jesa.530205

[48] Mathworks, "Matlab," 2020. https://www.mathworks.com/

[49] B. Choi, *Pulsewidth Modulated DC-to-DC Power Conversion*. Hoboken, NJ, USA: John Wiley & Sons, Inc., 2013.